

1 Metacommunity-scale biodiversity regulation and the self-organized
2 emergence of macroecological patterns

3 **Running Title:** Metacommunity-scale biodiversity regulation

4 Jacob D. O'Sullivan¹, Robert J. Knell¹, Axel G. Rossberg¹

5
6 ¹School of Biological and Chemical Sciences, Queen Mary University of London, Mile End Road, London, E1 4NS, United
7 Kingdom

8 **Corresponding author:** Jacob Dinner O'Sullivan, School of Biological and Chemical Sciences, Queen Mary University of
9 London, Mile End Road, London E1 4NS, United Kingdom, (j.l.dinner@qmul.ac.uk, +447402090620)

10 **Author contributions:** AGR conceived of the study. JDO and AGR designed the model. JDO developed the model,
11 performed simulations, analysed the data and drafted the manuscript. All three authors interpreted model outputs in comparison
12 with observations and contributed to manuscript writing. The authors declare no competing interests.

13 **Document statistics:** Abstract - 150 words, main text - 4836 words, supporting information 855 words, citations - 83,
14 main text figures - 6, supporting figures - 6

15 **Keywords:** biodiversity | macroecology | spatial ecology | metacommunity | ecological structural stability

16 Should this manuscript be accepted all simulation data supporting the results will be archived in a public repository and
17 the data DOI will be included at the end of the article

Abstract

19 There exist a number of key macroecological patterns whose ubiquity suggests the spatio-temporal structure
20 of ecological communities is governed by some universal mechanisms. The nature of these mechanisms, however,
21 remains poorly understood. Here we probe spatio-temporal patterns in species richness and community composition
22 using a simple metacommunity assembly model. Despite making no *a priori* assumptions regarding biotic spatial
23 structure or the distribution of biomass across species, model metacommunities self-organize to reproduce well
24 documented patterns including characteristic species abundance distributions, range size distributions and species
25 area relations. Also in agreement with observations, species richness in our model attains an equilibrium despite
26 continuous species turnover. Crucially, it is in the neighbourhood of the equilibrium that we observe the emergence of
27 these key macroecological patterns. Biodiversity equilibria in models occur due to the onset of ecological structural
28 instability, a population-dynamical mechanism. This strongly suggests a causal link between local community
29 processes and macroecological phenomena.

30 Introduction

31 Despite the colossal diversity of environments where life is found across the globe, there exist a number of spatio-temporal
32 patterns in biodiversity which are observed in almost every ecological community that has been studied. The species abundance
33 distribution (SAD), which highlights the overwhelming predominance of rare species in ecological communities, has long been
34 considered universal (Fisher et al., 1943; Preston, 1948). A related pattern, the range size distribution (RSD), points to the
35 prevalence of small (Brown et al., 1996; Gaston, 1996), aggregated (Brown, 1984) ranges, with few species occupying broad
36 distributions. The species area relation (SAR), which denotes the sub-linear increase in diversity as a function of sample area,
37 has been described as "one of community ecology's few genuine laws" (Schoener, 1976).

38 The less extensively studied (and considerably more divisive) phenomenon of community-level diversity regulation, which
39 constrains the number of species coexisting within an assemblage, has recently been proposed as a general ecological pattern
40 (Gotelli et al., 2017; Magurran et al., 2018). Evidence of strong diversity regulation has been found in desert rodents (Brown
41 et al., 2000), birds (Parody et al., 2001), marine fish (Magurran et al., 2015), freshwater communities (Magurran et al., 2018),
42 and in global-scale meta-analyses (Dornelas et al., 2014; Gotelli et al., 2017). At geological timescales, constrained diversification,
43 assumed to reflect the impact of ecological limits on evolutionary processes, has been detected in the fossil record of a variety
44 of taxa (Alroy, 2009, 2010; Liow and Finarelli, 2014; Benson et al., 2016; Close et al., 2019). Despite their apparent ubiquity,
45 which strongly hints at some almost universal processes in macroecology, our mechanistic understanding of these spatio-temporal
46 patterns in biodiversity remains disparate and incomplete.

47 The theory of island biogeography (MacArthur and Wilson, 1967) suggests that patterns in biodiversity may be explained
48 as a consequence of the dependence of diversification rates – speciation, invasion and extinction – on standing diversity. In the
49 fifty years since the Theory of Island Biogeography was first developed, however, the effects of environmental heterogeneity,
50 landscape topography, local species interactions and dispersal have been shown to impact local and regional diversity patterns
51 in complex ways (Shmida and Wilson, 1985; Holt, 1985; Pulliam, 1988). Contemporary metacommunity ecology (Leibold et al.,
52 2004; Holyoak et al., 2005; Logue et al., 2011; Winegardner et al., 2012) shines a light on how these complex and overlapping
53 processes interact. Perhaps due to the persistent view that local and regional ecological processes cannot be meaningfully
54 unified (Harmon and Harrison, 2015), surprisingly few studies consider metacommunity frameworks that explicitly incorporate
55 community dynamics at multiple spatial scales (e.g. Pillai et al., 2010; Barter and Gross, 2017; but see Plitzko and Drossel,
56 2015; Thiel and Drossel, 2018). Here we attempt to fill this gap with a dynamically simple metacommunity assembly model
57 which incorporates local ecological interactions and dispersal in an environmentally heterogeneous landscape, thus uniting the
58 branches of population-dynamical and spatial ecology. Our primary focus in developing this model was the study of how
59 biodiversity might be regulated in spatially resolved ecological assemblages, but we find an intriguing emergent relationship

60 between diversity regulation in model metacommunities and the appearance of widely observed macroecological patterns.

61 In spatially *unresolved* models, the emergence of biodiversity regulation has been observed numerous times (e.g. Drossel
62 et al., 2001; Yoshida, 2003; Pawar, 2009). Analytic theory (Rossberg, 2013) reveals that this phenomenon is caused by the loss
63 of *ecological structural stability*, which denotes the robustness of assemblages to press (i.e. sustained) perturbations (Meszena
64 et al., 2006; Bastolla et al., 2005, 2009; Rossberg, 2013; Rohr et al., 2014; Barbier et al., 2018). The mechanism is most easily
65 understood for the paradigmatic case of Lotka-Volterra competition models of the form

$$\frac{db_i}{dt} = \left(r_i - \sum_j^S \mathbf{A}_{ij} b_j \right) b_i \quad (1 \leq i \leq S), \quad (1)$$

66 with population biomasses b_i , linear growth rates r_i , competition coefficients $\mathbf{A}_{ij} \geq 0$, and species richness S . If all S species
67 co-exist ($b_i > 0$, for all i), the equilibrium condition for this system can be written in matrix-vector notation as $\mathbf{r} - \mathbf{A}\mathbf{b} = 0$
68 and is solved by $\mathbf{b} = \mathbf{A}^{-1}\mathbf{r}$. Mathematical problems of this form are called ‘ill conditioned’, implying that the solution \mathbf{b}
69 responds sensitively to changes in both \mathbf{A} and \mathbf{r} , when some eigenvalues of \mathbf{A} approach zero. In ecological models we define
70 this sensitivity as ecological structural *instability*. Once this unstable condition arises, perturbation by external pressures or
71 invaders, formally presentable by changes in \mathbf{A} or \mathbf{r} , can easily lead to extinctions. Structural stability (controlled by \mathbf{A}) and
72 linear/Lyapunov stability (controlled by the Jacobian matrix) should not be confused. While these two phenomena are related
73 (Stone, 2018), each of them can independently control community structure and dynamics.

74 Random matrix theory of the kind invoked by May (1973), but applied to the competition matrix \mathbf{A} rather than the system’s
75 Jacobian matrix at equilibrium, robustly predicts that with increasing species richness some eigenvalues of \mathbf{A} approach zero.
76 The overall effect is thus that with increasing species richness structural instability increases, and accordingly, the likelihood
77 that invasions cause species extinctions. Community assembly models therefore converge on dynamic steady states defined by
78 the onset of structural instability. By applying alternative mathematical approaches to studying this phenomenon (Yodzis, 1988;
79 Tokita, 2004; Rossberg, 2013; Dougoud et al., 2018; Barbier et al., 2018; Galla, 2018), structural instability can be interpreted
80 as resulting from the amplification of perturbations through complex indirect interactions in large communities.

81 For other types of spatially unresolved community models, approximation techniques have been developed to map these
82 onto competition models of the form Eq. (1) (layered food webs: Bastolla et al. 2005, mutualistic communities: Bastolla
83 et al. 2009, arbitrary food webs: Rossberg 2013), and the theory applies analogously. Whether this is similarly the case for
84 metacommunity models is unknown. In order to understand the relationship between diversity regulation, potentially via the
85 onset of ecological structural instability, and processes active in metacommunities, we constructed a multi-species framework
86 in which metapopulation dynamics at the regional scale are modelled using a spatial network of Lotka-Volterra competition
87 equations with additional terms describing dispersal (see *Dynamic equations and metacommunity assembly*, below).

88 By comparing the model’s behaviour to analytic predictions developed for spatially unresolved competitive communities
89 (Rossberg, 2013), we show that intrinsic metacommunity-level diversity regulation can indeed be explained as a consequence of
90 the onset of ecological structural instability at the *regional* scale. Surprisingly, and potentially very importantly, we find that, as
91 model metacommunities approach diversity limits, they *self organize* to reproduce macroecological patterns previously identified
92 as central for the spatial structure of biodiversity (McGill, 2010): a skewed local and regional distribution of abundances, spatial
93 aggregation of conspecific biomass, and apparent absence of species co-occurrence patterns. In combination, as McGill (2010)
94 argued, these core patterns lead to sub-linear species area relations and other spatial biodiversity phenomena. That a diverse
95 set of well known macroecological patterns emerges in a simple metacommunity model strongly supports the hypothesis that
96 these patterns are indeed indirect consequences of local, niche-based population dynamics and dispersal.

97 Results and discussion

98 Metacommunity species richness

99 Simulated metacommunities, assembled in our model via a constant, slow influx of invaders, converge on regional diversity
100 equilibria at which species richness remains approximately stationary despite continuous turnover in composition (Fig. 1).
101 Diversity relaxes back to the same approximate steady state after sudden removal or introduction of large numbers of species
102 (Fig. 1).

103 From previous theoretical work we know that the sensitivity of a spatially unresolved community to press perturbations is
104 a function of the standing diversity and the intensity of ecological interactions within that community (Rossberg, 2013). The
105 structurally unstable limit around which diversity in model communities converges, denoted S^* , is a function of the statistical
106 distribution of the competition coefficients, typically its first and second moments (mean, variance, covariances). By assuming
107 a precisely analogous mechanism to operate at the metacommunity scale, the basic spatially unresolved theory predicts an
108 approximate *regional* diversity of

$$S^* \approx \frac{(1 - E[\mathbf{C}_{ij}])^2}{2 \text{var}(\mathbf{C}_{ij})} \quad (i \neq j), \quad (2)$$

109 (Rossberg, 2013, Eq. 17.5) where $E[\mathbf{C}_{ij}]$ and $\text{var}(\mathbf{C}_{ij})$ represent the expectation and variance of the interspecific competition
110 coefficients computed at the scale of the metacommunity, replacing the distribution of local interaction coefficients \mathbf{A}_{ij} in the
111 spatially unresolved theory. The eigenvalue spectrum of the competitive overlap matrix offers a convenient graphical tool for
112 assessing the ecological structural stability of community models. The structurally unstable diversity limit occurs as the area
113 covered by the spectrum in the complex plane approach the origin (Rossberg, 2013).

114 Regional-scale, interspecific competition coefficients \mathbf{C}_{ij} were computed for model metacommunities assembled for a range
115 of parameter combinations, and used to evaluate Eq. (2) (see *Regional scale interaction matrices*, \mathbf{C} below). Comparing the
116 diversity predicted by Eq. (2) with that in the steady state of the simulation, we found that the spatially unresolved analytic
117 prediction explains 95% of variance in the equilibrium species richness in the spatially resolved models (Fig. 2A). Furthermore,
118 the spectra of the matrices \mathbf{C} approach the origin when the biodiversity equilibrium is reached (Fig. 2B), just as observed in
119 spatially unresolved models (Rossberg, 2013). Thus, although an analytic prediction of the structurally unstable diversity limit
120 in the metacommunity case is not available due to the intractability of the full model, we find strong evidence supporting the
121 claim that ecological structural stability drives diversity regulation at the metacommunity scale.

122 The relationship between local and regional competition coefficients is non-trivial and depends on the degree of environmental
123 heterogeneity (see *Model landscape*, below). Nonetheless, we found the off-diagonal elements of \mathbf{A}_{ij} and \mathbf{C}_{ij} to be significantly
124 correlated in metacommunity models at regional diversity limits ($p < 0.01$, for all parameter combinations). This implies that
125 local ecological interactions propagate to the metacommunity scale and influence regional diversity patterns (Rabosky and
126 Hurlbert, 2015). For further discussion see Supporting Information.

127 **Local species richness**

128 In order to distinguish between local and regional diversity it is necessary to define some criterion for assessing presence-absence
129 in a local assemblage. We do this in two ways. First by setting an arbitrary limit, equivalent to a detection threshold, of 10^{-4}
130 biomass units below which a species is considered to be absent from a local community. This value is four orders of magnitude
131 lower than the maximum local biomass permitted in the model and therefore defines a detectable range that is in accordance
132 with many empirical observations (e.g. Condit et al., 2002). We further distinguish among those populations exceeding the
133 detection threshold by defining *source* and *sink* populations as those capable of self maintenance in a given location, and those
134 that would decline without continuous immigration from adjacent communities (see *Source-Sink classification*, below).

135 During the assembly process (Fig. 1), we find that local community richness, defined by the detection threshold, saturates
136 earlier than the regional assemblage (after around ~ 500 and ~ 4000 invasions, respectively, in the example shown). To
137 confirm whether this local community regulation occurs independently of metacommunity regulation, it is necessary to ask how
138 α -diversity is related to γ -diversity. If local diversity limits are controlled indirectly by the size of the regional species pool
139 (i.e. regulation occurs meaningfully at one scale only) we would expect a linear, or at least non-saturating local-regional species
140 richness relation. Interestingly, however, both source and sink diversity, and, by extension, their sum, are saturating functions
141 of the regional species richness in equilibrium metacommunities. As we show in Fig. 3A, for which the distribution of interspecific
142 coefficients \mathbf{A}_{ij} was fixed across all simulations and considering source populations only, average local diversity converged on

143 a horizontal asymptote of ~ 50 once the regional assemblage reached ~ 300 species. Similar convergence, though with greater
144 scatter, is evident for sink populations, though the asymptote may occur outside of the range studied here. This suggests that
145 local diversity is indeed independently regulated, such that in sufficiently large regional communities local diversity is effectively
146 independent of the metacommunity-scale parameterization that determines the size of the regional species pool.

147 To explore the mechanism responsible for local diversity regulation we determined, for any given patch, the sub-matrix
148 of \mathbf{A} corresponding to the local source populations only. We found that the spectra of these sub-matrices, too, approach the
149 origin of the complex plane. Thus we concluded that structurally unstable dynamics regulate species richness not only at the
150 metacommunity level, but also, independently at the local level (Fig. 3B), and define sink populations as the super-saturated
151 component of the local assemblage which depends on non-equilibrium dynamics (mass effects) for persistence.

152 **Temporal turnover**

153 Stationarity in species richness is a key and unambiguous characteristic of our model metacommunities. Less obvious is the
154 fact that, rather than converging on a near-static, ‘climax’ community, metacommunity composition in our models continuously
155 turns over in response to the slow flux of invaders (Fig. 4A). Interestingly, on average, local communities turn over faster than
156 the regional metacommunity of which they form a part. This is seen in the rapid decay in community similarity at the local,
157 relative to the regional scale (Fig. 4A). This might be explained by range contraction and expansion due to regional biotic
158 turnover which occur faster than landscape-scale competitive exclusion.

159 If the invader flux is spontaneously stopped and species are experimentally removed from the metacommunity in increasing
160 order of regional biomass, fast turnover at local scales buffers local communities from the diversity losses at metacommunity
161 level (Fig. 4B). In the example shown in Fig. 4, a 20% decrease in regional species richness produced only a 13% drop at the
162 local scale on average. It has been estimated that the current rate of global species loss is 100-1000 times the background rate
163 (De Vos et al., 2015; Pimm et al., 2014; Ceballos et al., 2015), yet global meta-analyses have failed to detect a consistent loss of
164 diversity at the local scale (Dornelas et al., 2014; Vellend et al., 2017; Gotelli et al., 2017). Our results suggest that independent
165 regulatory processes operating at multiple spatial scales may account for the discrepancy between local and regional/global
166 diversity trends.

167 **Spatial patterns in biodiversity and abundance**

168 By elegantly comparing the various major efforts to devise unified macroecological theory to date, McGill (2010) showed that
169 three key macroecological phenomena are basic assumptions implicit to all frameworks. McGill argued that these key phenomena
170 on their own are sufficient to give rise to a variety of emergent macroecological patterns, such as the sub-linear SAR. The three

171 key patterns are an uneven SAD at various spatial scales, the spatial aggregation of conspecific biomass underlying the observed
172 skewed RSD, and the (apparent) non-significant correlation in species' spatial distributions. The last phenomenon relates to
173 the observation that statistically significant positive or negative correlations in species' spatial distributions or co-occurrence
174 patterns are surprisingly under-represented in empirical studies; most pair-wise correlations tend to be indistinguishable from
175 random (Hoagland and Collins, 1997; Veech, 2006; Houlihan et al., 2007; D'Amen et al., 2018). We find that, surprisingly, each
176 of these three patterns emerges in our model metacommunities in the neighbourhood of regional diversity equilibria (Fig. 5).

177 Figure 5A shows that at both local and regional scale the SAD are left-skewed log-normal, as observed in communities
178 ranging from marine benthos to Amazonian rain forest (McGill et al., 2007). The early onset of diversity regulation at the local
179 scale already leads to highly skewed SAD at the regional scale, after which further accumulation of diversity at the regional
180 scale drives the distribution to the left as average biomasses decline.

181 In the early stages of the assembly process, as local diversity accumulates, weak biotic filtering means species disperse across
182 much of their fundamental geographic niche. Once local communities become constrained, regional invasions instead drive an
183 increase in spatial β -diversity, the 'regionalization' of the biota (Ricklefs, 2004), and a corresponding reduction of species ranges,
184 which become highly spatially aggregated. At the metacommunity scale this is seen as a collapse in the RSD as the assemblage
185 approaches regional diversity equilibrium (Fig. 5B). The skewed RSD for metacommunity models at regional diversity limits
186 match patterns observed for a wide variety of taxa (Gaston, 1998), including pine species (Brown et al., 1996), tropical tree
187 species (Xu et al., 2015) and in both regional (Gaston, 1996), and global distributions (Orme et al., 2006) of bird species.
188 Reduction in average range sizes and the corresponding increase in the number of effective interactions with neighbouring
189 populations may increase species' vulnerability to regional extinction (Ricklefs, 2004). As such we consider the emergent spatial
190 aggregation in our metacommunity models to play an important role in regional scale diversity regulation.

191 The dependence of RSD on species richness implies a strong impact of ecological interactions on species ranges. Counter-intuitively,
192 however, the vast majority of species pairs show no significant spatial correlation (Fig. 5C). As strong regional scale diversity
193 regulation sets in and spatial ranges collapse, the percentage of species pairs for which it is possible to detect non-random spatial
194 correlation drops to near zero, giving the impression of an eminently neutral system.

195 We considered the possibility that this absence of demonstrable spatial correlations is explained by the systemic exclusion of
196 competing species pairs during assembly. However, for fully assembled model metacommunities at the regional diversity limit,
197 non-zero interspecific competition coefficients made up 21.5–28.3% of the elements of the matrix \mathbf{A}_{ij} , only 1.7–8.5% less than
198 in the statistical ensemble from which invaders are sampled.

199 McGill (2010) argues that these three key phenomena (Fig. 5) can combine to produce sub-linearity in the SAR. Recent
200 non-dynamical modelling approaches have also shown that local community processes and spatial aggregation at the population

201 scale can indeed generate high level macroecological configurations (Rogge et al., 2018; Takashina et al., 2019). Here we
202 build on these results by showing that explicitly modelled population dynamics can drive spatial aggregation and produce the
203 characteristic relationship between diversity and landscape area. The SAR in our models (Fig. 6) are well approximated by
204 power laws with exponents ranging from 0.19 to 0.87, depending on the degree of spatial correlation in the model environment:
205 a spatially more correlated, homogeneous environment produces an SAR with lower exponent. The exponents that emerge are
206 well within the range found in a meta-analysis of almost 800 empirical SARs (Drakare et al., 2006). It has been shown (Rosindell
207 and Cornell, 2007; Pigolotti et al., 2018) that realistic SAR emerge in spatially explicit neutral models. Here we show, in light
208 of evidence against neutral community assembly at regional scales (Ostling, 2005), how sublinearity in the SAR can emerge via
209 an explicit diversity dependent mechanism.

210 Conclusions

211 There is a growing body of evidence indicating that community level diversity regulation is a common characteristic of ecological
212 communities at both local and regional scales (e.g. Alroy, 2009; Magurran et al., 2015, 2018; Gotelli et al., 2017; Dornelas et al.,
213 2014). Proponents of this equilibrial paradigm concede that a precise mechanism explaining community regulation remains
214 elusive (Magurran et al., 2018). Our numerical metacommunity model hints at a potential resolution to this problem and
215 highlights an important avenue for the development of novel analytic theory. Inspection of recent results by Abernethy et al.
216 (2019) for a spatially explicit food-web model in the light of our observations suggests that the phenomena we observe are not
217 restricted to competitive communities, but may apply to a wider range of ecological models.

218 With this study we set out to assess the degree to which spatially unresolved ecological theory can incorporate the complex
219 spatial processes occurring within model metacommunities. To our surprise, metacommunity models which explicitly incorporate
220 dynamics at both local and regional scales reproduce an unprecedented range of empirically ubiquitous macroecological patterns.
221 Crucially, these patterns result indirectly from the local dynamics, and in the neighbourhood of regional diversity limits. From
222 this observation we conclude that there is an important interaction between the system-scale dynamical process central to the
223 theory of ecological structural stability, and these key macroecological configurations. The spatial decoupling of timescales we
224 observe (Fig 4A) implies that for a metacommunity of sufficiently large spatial extent regional ecological turnover could occur
225 at time scales comparable to evolutionary or long-term environmental processes (e.g. glaciation cycles), as discussed by Ricklefs
226 (2004). Because these processes are not include in our model, the 'regional' scale we refer to here must be understood as an
227 intermediate spatial scale at which ecological processes operate comparatively fast.

228 If we conclude, on the basis of this and similar studies, that diversity regulation is indeed a common or general feature of

229 ecological communities, this would entail a paradigm shift with important implications for the conservation and management
230 of biodiversity. The assumption that local ecological dynamics have negligible impact on regional biotic distributions is still
231 implicit in the majority of current conservation policies and programs. Species distribution modelling (SDM) is a widely
232 used method for identifying ecological processes and responses of species distributions to environmental change. The basic
233 SDM methodology assumes a comprehensive understanding of current and future climate is sufficient to predict range shifts
234 under climate change. Our results suggest that ignoring biotic interactions, even if they cannot be explicitly detected using
235 conventional tools, may strongly undermine the effectiveness of these models (Wisiz et al., 2013). As such, we suggest that
236 the development and application of more mechanistic distribution modelling (Dormann et al., 2018) should be a priority, that
237 management models might focus on higher levels of biological organisation (e.g. feeding guilds or entire communities), and that
238 designers of conservation and management strategies make a concerted effort to integrate factors relating to diversity regulation
239 in their decision making.

240 **Methods**

241 **Model landscape**

242 We generated a spatial network consisting of N patches by sampling the Cartesian coordinates (P_x, Q_x) of each patch x (with
243 $1 \leq x \leq N$) from a uniform distribution in the range $(0, \sqrt{N})$. The local communities, were thus randomly distributed with
244 density ≈ 1 over a model landscape of area N . Corridors were defined using the Gabriel algorithm (1969) which connects nodes
245 x and y if the disc with diameter given by the line segment \overline{xy} contains no other nodes. This non-trivial topography is more
246 realistic than a complete graph, but was also selected for its relative computational efficiency. In the limit of large N , the average
247 patch degree does not exceed 4 (Matula and Sokal, 1980), as for a square lattice, which will permit implementation of parallel
248 simulation methods currently under development. Numerical experiments with fully connected graph lead to qualitatively
249 similar emergent properties (see Supporting Information).

250 Environmental heterogeneity was modelled indirectly through spatial variation in species' intrinsic growth rates r_{ix} , where
251 the subscript i is a species index, and x a patch index. The species specific distribution in r_{ix} represents the output of an
252 implicit environmental response function, that, if explicitly modelled, would describe a population's maximum growth rate at
253 low abundance (i.e. in the absence of competition) as a function of species traits and local environmental conditions. The values
254 of r_{ix} were sampled from a Gaussian Random Field (Adler, 1981) ($\mu = 1.0$, $\sigma^2 = 0.5$), generated via spectral decomposition of the
255 N by N landscape covariance matrix with elements $\Sigma_{L,xy} = \exp[-\phi^{-1}d_{xy}]$, where d_{xy} denotes the Euclidean distances between
256 two patches x and y , and the parameter ϕ controls the spatial autocorrelation of the environment (Johnson and Wichern, 2002).

257 By varying the correlation length ϕ while keeping mean and variance of the fields fixed, we modelled landscapes of varying
 258 degrees of environmental heterogeneity (see Supporting Information), thus though the environment is not modelled, the spatial
 259 autocorrelation in environmental variables is explicit in the vector \mathbf{r}_{ix} . Parameters were chosen as $N = 10$, $\phi = 1$ for Fig. 1,
 260 $N = 20$, $\phi = 1$ for Figs. 4 and 5. (Temporal decoupling of spatial scales is clearer in larger regional communities, however for
 261 γ -diversity $\gg \alpha$ -diversity it becomes difficult to represent local and regional assemblages on a single axis.) Figs. 2, 3, and 6
 262 summarize the complete parameter space studied: $N = 2, 4, 6, 8, 10, 12, 15, 20$, and 25; $\phi = 1, 2, 5, 10, 20, 40, 80$, and 160,
 263 in all combinations. Landscapes of $\phi > 160$ (in the spatial range studied here) showed no further decrease in *gamma*, or the
 264 exponent of the SAR, implying an effectively uniform environment.

265 Dynamic equations and metacommunity assembly

266 We used a spatial extension of the Lotka-Volterra multi-species competition equation to model local population dynamics and
 267 dispersal in our model metacommunities, thus building on the model family pioneered by Reichenbach et al. (2007). The rate
 268 of change of local biomass of species i at patch x is given by the non-linear ordinary differential equation

$$\begin{aligned} \frac{db_{ix}}{dt} = & b_{ix} \left(r_{ix} - \sum_{j=1}^S \mathbf{A}_{ij} b_{jx} \right) - e b_{ix} \\ & + \sum_{y \in \mathcal{N}(x)} \frac{e}{k_y} \exp(-d_{xy} \ell^{-1}) b_{iy}. \end{aligned} \quad (3)$$

269 The system of $N \times S$ coupled equations can therefore be written as

$$\frac{d\mathbf{B}}{dt} = \mathbf{B} \circ (\mathbf{R} - \mathbf{A}\mathbf{B}) + \mathbf{B}\mathbf{D}, \quad (4)$$

270 with \circ denoting element-wise multiplication.

271 The first term on the right hand side of Eq. (3) represents the local dynamics, where \mathbf{A}_{ij} are the entries of the spatially
 272 unresolved competitive overlap matrix. In simulations, the off-diagonal entries \mathbf{A}_{ij} were sampled randomly, with \mathbf{A}_{ij} set to
 273 0.3 with probability 0.3 and to 0 otherwise. The diagonal entries, representing intraspecific competition, were always set to
 274 1. Together, Eq. (2) and Fig. 2 imply that the critical diversity at which a model community converges depends only on the
 275 expectation and variance of the regional interspecific interaction coefficients. The details of the distribution from which the \mathbf{A}_{ij}
 276 are sampled do not enter the spatially implicit theory. For interaction matrices with pronounced structure (e.g. food webs),
 277 however, the underlying theory breaks down Rossberg (2013). The impact of the fundamental distribution from which the local

278 interactions \mathbf{A}_{ij} are sampled on spatial diversity patterns is subject of ongoing research.

279 The second term on the right of Eq. (3) represents the rate at which biomass of species i emigrates away from patch x ,
280 while the third term gives the immigration rates from all patches y sharing an edge with x . The immigration rate decays
281 exponentially with characteristic length ℓ , kept fixed at 0.2. The parameter e , which represents the fraction of biomass leaving
282 patch x per unit time, was kept fixed at 0.02. An exploration of the parameter space of e and ℓ revealed little qualitative shift
283 in the emergent properties of the model over the biologically relevant range (see Supporting Information), thus values were
284 selected that favoured computational efficiency during model assembly. The normalization constant k_y divides the biomass
285 departing patches y between all other patches in the *its* local neighbourhood ($\mathcal{N}(y)$), weighted by the ease of reaching each
286 patch i.e. $k_y = \sum_{z \in \mathcal{N}(y)} \exp(-d_{yz} \ell^{-1})$.

287 We adopted the community assembly modelling approach first developed by Post and Pimm (1983). In each iteration of
288 the algorithm, a new species was added to the metacommunity. Invaders were selected by computing the effective growth rate
289 at low abundance of new species i with randomly generated ecologies (r_{ix} and \mathbf{A}_{ij}), until a species with positive growth rate
290 in at least one patch was found. This was then added to the patch in which its effective growth rate was greatest with a low
291 invasion biomass of 0.01 times the detection threshold of 10^{-4} biomass units. During invader testing the competitive impact
292 of the invader on the dynamics of resident species was set to zero, such that resident biomass was unaffected, to make sure
293 we capture the invader's linear dynamics at low abundance. The metacommunity dynamics, including the spread of the new
294 invader through the network and associated restructuring the local resident biomass distribution, were then simulated using the
295 SUNDIALS numerical ODE solver (Hindmarsh et al., 2005) over 500 unit times, t . Those species whose biomass dropped below
296 the detection threshold in all patches of the network were considered regionally extinct and removed from the system. By thus
297 iteratively adding species to the community we modelled a constant flux of invaders, which causes the regional assemblage to
298 self-organize, eventually converging on an equilibrium at which the invasion and extinction rates are equal on average. To reach
299 this equilibrium, total simulation time was chosen as 4000, 6000, 8000, 10000, and 12000 iterations for $N \leq 4$, $6 \leq N \leq 10$,
300 $12 \leq N \leq 15$, $N = 20$ and $N = 25$, respectively.

301 We note that \sqrt{N} determines the linear extension of the system, while ϕ and ℓ represent intrinsic length scales. There is a
302 third intrinsic length scales, given by $1/\sqrt{\text{density of patches}}$, and this scale we kept fixed at 1. Because of this, there is no easy
303 way to eliminate variables by re-scaling lengths. It is conceivable that for very large system sizes N the discrete patch structure
304 can give way to a continuum approximation with less parameters, but the question whether this is the case is beyond the scope
305 of the present work.

306 Source-Sink classification

307 Source populations in a given patch x are those capable of locally maintaining themselves. Mathematically, source populations
308 were defined as those for which local biomass was greater than the detection threshold and $r_{ix} - \sum_{j=1}^S \mathbf{A}_{ij} b_{jx} \geq 0$. Conversely,
309 sink populations were those of biomass greater than the detection threshold and $r_{ix} - \sum_{j=1}^S \mathbf{A}_{ij} b_{jx} < 0$.

310 Regional scale interaction matrices, \mathbf{C}

311 In order to compare model metacommunity dynamics to theoretical predictions, we numerically computed a spatially unresolved
312 competitive overlap matrix, denoted \mathbf{C} , that summarized the macroscopic dynamics at the regional scale. For this we constructed
313 a spatially *unresolved* Lotka-Volterra system,

$$d\mathbf{B}_i/dt = \left(\rho_i - \sum_{j=1}^S \hat{\mathbf{C}}_{ij} \mathbf{B}_j \right) \cdot \mathbf{B}_i, \quad (5)$$

314 where \mathbf{B}_i represents total biomass of species i , as an approximation of the spatially *resolved* model (Eq. (3)). The aim of
315 the following method is to arrive at a description of the effective interaction between pairs of species given the self-organized
316 spatial structure of metacommunity, which permits regional coexistence via spatial niche segregation. This requires integrating
317 ecological interactions over the entire landscape, which was done using the computational equivalent of a harvesting experiment,
318 under the assumption that interaction strengths can be inferred from the changes in regional abundances that result from
319 controlled changes in the regional abundances of harvested species (Gilbert et al., 2014). Specifically, we asked how the steady
320 state community responds to spatially unselective, light harvesting of a single species in the full model, and determined the
321 coefficients $\hat{\mathbf{C}}_{ij}$ of the unresolved model such as to obtain identical responses to linear order in the harvesting rate.

$$\Delta \mathbf{B}_j = -\hat{\mathbf{C}}_{ij}^{-1} h. \quad (6)$$

322 The most computationally efficient way of conducting the corresponding experiment for the meta-community is to use a
323 numerical approximation of the Jacobian matrix. In doing so, we assume simulated metacommunities to be at fixed points, an
324 approximation that is justified retrospectively by the apparent efficacy of the method. In fact, large metacommunity models
325 begin to manifest periodic or irregular oscillations, a potentially important phenomenon which is the subject of ongoing research.
326 For the present study we limited our numerical experiments to those spatial ranges in which such autonomous fluctuations are
327 absent or weak, such that the numerical Jacobian represents a reasonable approximation of the dynamic coupling within the
328 system and can be used to compute a time-independent, regional scale interaction matrix which meaningfully describes the
329 structural stability of the metacommunity. The elements of the Jacobian are given by the general equation

$$\mathbf{J}_{ixjy} = \frac{\partial f_{ix}(b_{11}, \dots, b_{S1}, \dots, b_{1N}, \dots, b_{SN})}{\partial b_{jy}}, \quad (7)$$

330 evaluated at equilibrium. The functions f_{ix} denote the right hand side of Eq. (3).

331 Light harvesting of a single focal species i at a rate h brings about a small shift in the equilibrium biomasses of the other
 332 species in the metacommunity and the dynamics of the harvested community *near the unharvested equilibrium* (b_{jy}^*) can be
 333 approximated by

$$\frac{db_{ix}}{dt} = \left(\sum_{jy} \mathbf{J}_{ixjy} (b_{jy} - b_{jy}^*) \right) - hb_{ix}^*, \quad \text{and} \quad (8a)$$

334

$$\frac{db_{kx}}{dt} = \left(\sum_{jy} \mathbf{J}_{kxjy} (b_{jy} - b_{jy}^*) \right) \quad \text{for } k \neq i. \quad (8b)$$

335 Here h is the harvesting rate. We vectorize the matrix \mathbf{B} (denoted $\vec{\mathbf{B}}$) such as to match the dimensionality of the spatially
 336 resolved Jacobian, and we write the equilibrium condition for Eq. (8a) as

$$\mathbf{J}(\vec{\mathbf{B}} - \vec{\mathbf{B}}^*) - \vec{\mathbf{H}} = 0, \quad (9)$$

337 where the elements of vector $\vec{\mathbf{H}}$ are hb_{jy}^* for $j = i$ and 0 otherwise. From this, we obtain

$$h^{-1}(\vec{\mathbf{B}} - \vec{\mathbf{B}}^*) = \mathbf{J}^{-1}h^{-1}\vec{\mathbf{H}}. \quad (10)$$

338 The left hand side of Eq. (10) represents the local shift in biomasses due to the harvesting of the focal species i per unit h .
 339 From Eq. (10) we compute the change in total biomass $\Delta \mathbf{B}_j = \sum_x b_{jx} - b_{jx}^*$ for each species j . Comparison with (6) gives row
 340 i of $\hat{\mathbf{C}}^{-1}$. Iterating over all species $i = 1 \dots S$, we computed $\hat{\mathbf{C}}^{-1}$ and from this the spatially unresolved interaction matrix $\hat{\mathbf{C}}$.
 341 Finally, in order to match the assumptions made in the derivation of Eq. (2) (Rossberg, 2013), we divided each row and column
 342 $\hat{\mathbf{C}}$ by the square root of the corresponding diagonal element to obtain the *effective competitive overlap matrix*, \mathbf{C} (which has
 343 ones along the diagonal).

344 Temporal diversity patterns

345 Temporal species richness and turnover in community composition were computed for a metacommunity at regional diversity
 346 limits for a period corresponding to 500 ecological invasions (Fig. 4). Species richness analysis requires the application of
 347 some presence-absence criterion. We assess local community diversity by reference to the source populations only, since sink
 348 populations are effectively decoupled from local filtering processes by dispersal.

349 Following the 500 invasions, species were removed in reverse order of regional abundance, in order to model a large scale
 350 mass extinction process. A single metacommunity of $N = 20$, $\phi = 2$ was used for this analysis.

351 Compositional turnover in metacommunities at regional diversity equilibria was measured using the Bray-Curtis (1957)
 352 similarity. An arbitrary initial metacommunity composition was selected ($T = 0$ in Fig. 4A) and the relative compositional
 353 change computed in the context of a constant invasion flux using the function `vegdist` in the R package “vegan” (Oksanen
 354 et al., 2018). In order to generate Fig. 4A, regionally excluded or as yet uninvaded species were assigned biomass vectors with
 355 all elements set to zero.

356 Species ranges

357 In order to quantify range sizes of species, we first computed, for each species, the population covariance matrix

$$\Sigma_i = \begin{pmatrix} \text{var}(P_x) & \text{cov}(P_x, Q_x) \\ \text{cov}(P_x, Q_x) & \text{var}(Q_x) \end{pmatrix} \quad (11)$$

358 of the locations (P_x, Q_x) of individuals forming the species’ population, assuming population sizes are proportional to biomasses
 359 at each patch. For example, with i being the index of the focal species, $\text{var}(P_x) = \mathbf{B}_i^{-1} \sum_x b_{ix} (P_x - \bar{P}_x)^2$, where $\mathbf{B}_i = \sum_x b_{ix}$ is
 360 total biomass, as above, and $\bar{P}_x = \mathbf{B}_i^{-1} \sum_x b_{ix} P_x$ is the P component of the centre of mass of the distribution. Correspondingly,
 361 $\text{var}(Q_x) = \mathbf{B}_i^{-1} \sum_x b_{ix} (Q_x - \bar{Q}_x)^2$, $\text{cov}(P_x, Q_x) = \mathbf{B}_i^{-1} \sum_x b_{ix} (P_x - \bar{P}_x)(Q_x - \bar{Q}_x)$, with $\bar{Q}_x = \mathbf{B}_i^{-1} \sum_x b_{ix} Q_x$. As a measure
 362 of range size, we computed the product of the square roots of the eigenvalues of Σ_i , i.e. the square root of its determinant,
 363 $\sqrt{\det|\Sigma_i|}$. By this measure, an even distribution of biomass over the full $\sqrt{N} \times \sqrt{N}$ rectangle enclosing one of our model
 364 communities corresponds to a range size of $N/12$.

365 Species co-occurrence

366 In order to analyse the correlation in species spatial distributions within our model landscapes, we used the probabilistic model
 367 developed by Veech (2013) included in the R package “cooccur” (Griffith et al., 2016). The observed pair-wise co-occurrence is
 368 computed as the probability of detecting species i in patch x given the detection of species j in that local community, which is
 369 then compared to that expected if two species were distributed independently within a discretized landscape.

370 References

- 371 G. M. Abernethy, M. McCartney, and D. H. Glass. The role of migration in a spatial extension of the webworld eco-evolutionary
372 model. *Ecological Modelling*, 397:122–140, 2019.
- 373 R. J. Adler. *The geometry of random fields*, volume 62. Siam, 1981.
- 374 J. Alroy. Speciation and extinction in the fossil record of north american mammals. In R. Butlin, J. Bridle, and D. Schluter,
375 editors, *Speciation and patterns of diversity*, chapter 16. Cambridge University Press, 2009.
- 376 J. Alroy. Geographical, environmental and intrinsic biotic controls on phanerozoic marine diversification. *Palaeontology*, 53(6):
377 1211–1235, 2010.
- 378 M. Barbier, J.-F. Arnoldi, G. Bunin, and M. Loreau. Generic assembly patterns in complex ecological communities. *PNAS*,
379 page 201710352, Feb. 2018. ISSN 0027-8424, 1091-6490. doi: 10.1073/pnas.1710352115.
- 380 E. Barter and T. Gross. Spatial effects in meta-foodwebs. *Scientific Reports*, 7(1):9980, 2017.
- 381 U. Bastolla, M. Lässig, S. C. Manrubia, and A. Valleriani. Biodiversity in model ecosystems, i: coexistence conditions for
382 competing species. *Journal of Theoretical Biology*, 235(4):521–530, 2005.
- 383 U. Bastolla, M. A. Fortuna, A. Pascual-García, A. Ferrera, B. Luque, and J. Bascompte. The architecture of mutualistic
384 networks minimizes competition and increases biodiversity. *Nature*, 458(7241):1018, 2009.
- 385 R. B. Benson, R. J. Butler, J. Alroy, P. D. Mannion, M. T. Carrano, and G. T. Lloyd. Near-stasis in the long-term diversification
386 of mesozoic tetrapods. *PLoS biology*, 14(1):e1002359, 2016.
- 387 J. R. Bray and J. T. Curtis. An ordination of the upland forest communities of southern wisconsin. *Ecological monographs*, 27
388 (4):325–349, 1957.
- 389 J. H. Brown. On the relationship between abundance and distribution of species. *The american naturalist*, 124(2):255–279,
390 1984.
- 391 J. H. Brown, G. C. Stevens, and D. M. Kaufman. The geographic range: size, shape, boundaries, and internal structure. *Annual*
392 *review of ecology and systematics*, 27(1):597–623, 1996.
- 393 J. H. Brown, S. M. Ernest, J. M. Parody, and J. P. Haskell. Regulation of diversity: maintenance of species richness in changing
394 environments. *Oecologia*, 126(3):321–332, 2000.

395 G. Ceballos, P. R. Ehrlich, A. D. Barnosky, A. García, R. M. Pringle, and T. M. Palmer. Accelerated modern human-induced
396 species losses: Entering the sixth mass extinction. *Science advances*, 1(5):e1400253, 2015.

397 R. A. Close, R. B. Benson, J. Alroy, A. K. Behrensmeyer, J. Benito, M. T. Carrano, T. J. Cleary, E. M. Dunne, P. D. Mannion,
398 M. D. Uhen, et al. Diversity dynamics of phanerozoic terrestrial tetrapods at the local-community scale. *Nature Ecology &*
399 *Evolution*, page 1, 2019.

400 R. Condit, N. Pitman, E. G. Leigh, J. Chave, J. Terborgh, R. B. Foster, P. Núñez, S. Aguilar, R. Valencia, G. Villa, et al.
401 Beta-diversity in tropical forest trees. *Science*, 295(5555):666–669, 2002.

402 M. D’Amen, H. K. Mod, N. J. Gotelli, and A. Guisan. Disentangling biotic interactions, environmental filters, and dispersal
403 limitation as drivers of species co-occurrence. *Ecography*, 41(8):1233–1244, 2018.

404 J. M. De Vos, L. N. Joppa, J. L. Gittleman, P. R. Stephens, and S. L. Pimm. Estimating the normal background rate of species
405 extinction. *Conservation Biology*, 29(2):452–462, 2015.

406 C. F. Dormann, M. Bobrowski, D. M. Dehling, D. J. Harris, F. Hartig, H. Lischke, M. D. Moretti, J. Pagel, S. Pinkert,
407 M. Schleuning, et al. Biotic interactions in species distribution modelling: 10 questions to guide interpretation and avoid
408 false conclusions. *Global Ecology and Biogeography*, 2018.

409 M. Dornelas, N. J. Gotelli, B. McGill, H. Shimadzu, F. Moyes, C. Sievers, and A. E. Magurran. Assemblage time series reveal
410 biodiversity change but not systematic loss. *Science*, 344(6181):296–299, 2014.

411 M. Dougoud, L. Vinckenbosch, R. P. Rohr, L.-F. Bersier, and C. Mazza. The feasibility of equilibria in large ecosystems: A
412 primary but neglected concept in the complexity-stability debate. *PLOS Computational Biology*, 14(2):e1005988, 2018. ISSN
413 1553-7358. doi: 10.1371/journal.pcbi.1005988.

414 S. Drakare, J. J. Lennon, and H. Hillebrand. The imprint of the geographical, evolutionary and ecological context on species–area
415 relationships. *Ecology letters*, 9(2):215–227, 2006.

416 B. Drossel, P. G. Higgs, and A. J. McKane. The influence of predator–prey population dynamics on the long-term evolution of
417 food web structure. *Journal of Theoretical Biology*, 208(1):91–107, 2001.

418 R. A. Fisher, A. S. Corbet, and C. B. Williams. The relation between the number of species and the number of individuals in
419 a random sample of an animal population. *The Journal of Animal Ecology*, pages 42–58, 1943.

420 K. R. Gabriel and R. R. Sokal. A new statistical approach to geographic variation analysis. *Systematic zoology*, 18(3):259–278,
421 1969.

422 T. Galla. Dynamically evolved community size and stability of random Lotka-Volterra ecosystems(a). *EPL*, 123(4):48004, Sept.
423 2018. ISSN 0295-5075. doi: 10.1209/0295-5075/123/48004.

424 K. J. Gaston. Species-range-size distributions: patterns, mechanisms and implications. *Trends in Ecology & Evolution*, 11(5):
425 197–201, 1996.

426 K. J. Gaston. Species-range size distributions: products of speciation, extinction and transformation. *Philosophical Transactions*
427 *of the Royal Society B: Biological Sciences*, 353(1366):219–230, 1998.

428 B. Gilbert, T. D. Tunney, K. S. McCann, J. P. DeLong, D. A. Vasseur, V. Savage, J. B. Shurin, A. I. Dell, B. T. Barton,
429 C. D. Harley, et al. A bioenergetic framework for the temperature dependence of trophic interactions. *Ecology Letters*, 17
430 (8):902–914, 2014.

431 N. J. Gotelli, H. Shimadzu, M. Dornelas, B. McGill, F. Moyes, and A. E. Magurran. Community-level regulation of temporal
432 trends in biodiversity. *Science advances*, 3(7):e1700315, 2017.

433 D. M. Griffith, J. A. Veech, C. J. Marsh, et al. cooccur: Probabilistic species co-occurrence analysis in r. *J Stat Softw*, 69(2):
434 1–17, 2016.

435 L. J. Harmon and S. Harrison. Species diversity is dynamic and unbounded at local and continental scales. *The American*
436 *Naturalist*, 185(5):584–593, 2015.

437 A. C. Hindmarsh, P. N. Brown, K. E. Grant, S. L. Lee, R. Serban, D. E. Shumaker, and C. S. Woodward. Sundials: Suite of
438 nonlinear and differential/algebraic equation solvers. *ACM Transactions on Mathematical Software (TOMS)*, 31(3):363–396,
439 2005.

440 B. W. Hoagland and S. L. Collins. Gradient models, gradient analysis, and hierarchical structure in plant communities. *Oikos*,
441 pages 23–30, 1997.

442 R. D. Holt. Population dynamics in two-patch environments: some anomalous consequences of an optimal habitat distribution.
443 *Theoretical population biology*, 28(2):181–208, 1985.

444 M. Holyoak, M. A. Leibold, and R. D. Holt. *Metacommunities: spatial dynamics and ecological communities*. University of
445 Chicago Press, 2005.

446 J. E. Houlahan, D. J. Currie, K. Cottenie, G. S. Cumming, S. Ernest, C. S. Findlay, S. D. Fuhlendorf, U. Gaedke, P. Legendre,
447 J. J. Magnuson, et al. Compensatory dynamics are rare in natural ecological communities. *Proceedings of the National*
448 *Academy of Sciences*, 104(9):3273–3277, 2007.

449 R. A. Johnson and D. Wichern. *Multivariate analysis*. Wiley Online Library, 2002.

450 M. A. Leibold, M. Holyoak, N. Mouquet, P. Amarasekare, J. M. Chase, M. F. Hoopes, R. D. Holt, J. B. Shurin, R. Law,
451 D. Tilman, et al. The metacommunity concept: a framework for multi-scale community ecology. *Ecology letters*, 7(7):
452 601–613, 2004.

453 L. H. Liow and J. A. Finarelli. A dynamic global equilibrium in carnivoran diversification over 20 million years. In *Proc. R.*
454 *Soc. B*, volume 281. The Royal Society, 2014.

455 J. B. Logue, N. Mouquet, H. Peter, H. Hillebrand, M. W. Group, et al. Empirical approaches to metacommunities: a review
456 and comparison with theory. *Trends in ecology & evolution*, 26(9):482–491, 2011.

457 R. H. MacArthur and E. O. Wilson. *The theory of island biogeography*. Princeton, NJ, 1967.

458 A. E. Magurran, M. Dornelas, F. Moyes, N. J. Gotelli, and B. McGill. Rapid biotic homogenization of marine fish assemblages.
459 *Nature communications*, 6:8405, 2015.

460 A. E. Magurran, A. E. Deacon, F. Moyes, H. Shimadzu, M. Dornelas, D. A. Phillip, and I. W. Ramnarine. Divergent biodiversity
461 change within ecosystems. *Proceedings of the National Academy of Sciences*, page 201712594, 2018.

462 D. W. Matula and R. R. Sokal. Properties of gabriel graphs relevant to geographic variation research and the clustering of
463 points in the plane. *Geographical analysis*, 12(3):205–222, 1980.

464 R. M. May. *Stability and complexity in model ecosystems*. Princeton university press, 1973.

465 B. J. McGill. Towards a unification of unified theories of biodiversity. *Ecology letters*, 13(5):627–642, 2010.

466 B. J. McGill, R. S. Etienne, J. S. Gray, D. Alonso, M. J. Anderson, H. K. Benecha, M. Dornelas, B. J. Enquist, J. L. Green,
467 F. He, et al. Species abundance distributions: moving beyond single prediction theories to integration within an ecological
468 framework. *Ecology letters*, 10(10):995–1015, 2007.

469 G. Meszéna, M. Gyllenberg, L. Pásztor, and J. A. Metz. Competitive exclusion and limiting similarity: a unified theory.
470 *Theoretical Population Biology*, 69(1):68–87, 2006.

471 J. Oksanen, F. G. Blanchet, M. Friendly, R. Kindt, P. Legendre, D. McGlinn, P. R. Minchin, R. B. O'Hara, G. L.
472 Simpson, P. Solymos, M. H. H. Stevens, E. Szoecs, and H. Wagner. *vegan: Community Ecology Package*, 2018. URL
473 <https://CRAN.R-project.org/package=vegan>. R package version 2.4-6.

474 C. D. L. Orme, R. G. Davies, V. A. Olson, G. H. Thomas, T.-S. Ding, P. C. Rasmussen, R. S. Ridgely, A. J. Stattersfield, P. M.
475 Bennett, I. P. Owens, et al. Global patterns of geographic range size in birds. *PLoS biology*, 4(7):e208, 2006.

476 A. Ostling. Ecology: Neutral theory tested by birds. *Nature*, 436(7051):635, 2005.

477 J. M. Parody, F. J. Cuthbert, and E. H. Decker. The effect of 50 years of landscape change on species richness and community
478 composition. *Global Ecology and Biogeography*, 10(3):305–313, 2001.

479 S. Pawar. Community assembly, stability and signatures of dynamical constraints on food web structure. *Journal of theoretical*
480 *biology*, 259(3):601–612, 2009.

481 S. Pigolotti, M. Cencini, D. Molina, and M. A. Muñoz. Stochastic spatial models in ecology: a statistical physics approach.
482 *Journal of Statistical Physics*, 172(1):44–73, 2018.

483 P. Pillai, M. Loreau, and A. Gonzalez. A patch-dynamic framework for food web metacommunities. *Theoretical Ecology*, 3(4):
484 223–237, 2010.

485 S. L. Pimm, C. N. Jenkins, R. Abell, T. M. Brooks, J. L. Gittleman, L. N. Joppa, P. H. Raven, C. M. Roberts, and J. O.
486 Sexton. The biodiversity of species and their rates of extinction, distribution, and protection. *Science*, 344(6187):1246752,
487 2014.

488 S. J. Pitzko and B. Drossel. The effect of dispersal between patches on the stability of large trophic food webs. *Theoretical*
489 *Ecology*, 8(2):233–244, 2015.

490 W. Post and S. Pimm. Community assembly and food web stability. *Mathematical Biosciences*, 64(2):169–192, 1983.

491 F. W. Preston. The commonness, and rarity, of species. *Ecology*, 29(3):254–283, 1948.

492 H. R. Pulliam. Sources, sinks, and population regulation. *The American Naturalist*, 132(5):652–661, 1988.

493 D. L. Rabosky and A. H. Hurlbert. Species richness at continental scales is dominated by ecological limits. *The American*
494 *Naturalist*, 185(5):572–583, 2015.

- 495 T. Reichenbach, M. Mobilia, and E. Frey. Mobility promotes and jeopardizes biodiversity in rock–paper–scissors games. *Nature*,
496 448(7157):1046, 2007.
- 497 R. E. Ricklefs. A comprehensive framework for global patterns in biodiversity. *Ecology letters*, 7(1):1–15, 2004.
- 498 T. Rogge, D. Jones, B. Drossel, and K. T. Allhoff. Interplay of spatial dynamics and local adaptation shapes species lifetime
499 distributions and species–area relationships. *Theoretical Ecology*, pages 1–15, 2018.
- 500 R. P. Rohr, S. Saavedra, and J. Bascompte. On the structural stability of mutualistic systems. *Science*, 345(6195):1253497,
501 2014.
- 502 J. Rosindell and S. J. Cornell. Species–area relationships from a spatially explicit neutral model in an infinite landscape. *Ecology*
503 *letters*, 10(7):586–595, 2007.
- 504 A. G. Rossberg. *Food webs and biodiversity: foundations, models, data*. John Wiley & Sons, 2013.
- 505 T. Schoener. The species-area relation within archipelagos: models and evidence from island land birds. In *16th International*
506 *Ornithological Congress, Canberra, Australia, 12 to 17 August 1974*, pages 629–642. Australian Academy of Sciences, 1976.
- 507 A. Shmida and M. V. Wilson. Biological determinants of species diversity. *Journal of biogeography*, pages 1–20, 1985.
- 508 L. Stone. The feasibility and stability of large complex biological networks: A random matrix approach. *Sci. Rep.*, 8(1):8246,
509 May 2018. ISSN 2045-2322. doi: 10.1038/s41598-018-26486-2.
- 510 N. Takashina, B. Kusumoto, Y. Kubota, and E. P. Economo. A geometric approach to scaling individual distributions to
511 macroecological patterns. *Journal of theoretical biology*, 461:170–188, 2019.
- 512 T. Thiel and B. Drossel. Impact of stochastic migration on species diversity in meta-food webs consisting of several patches.
513 *Journal of theoretical biology*, 443:147–156, 2018.
- 514 K. Tokita. Species abundance patterns in complex evolutionary dynamics. *Phys. Rev. Lett.*, 93:178102, 2004.
- 515 J. A. Veech. A probability-based analysis of temporal and spatial co-occurrence in grassland birds. *Journal of Biogeography*,
516 33(12):2145–2153, 2006.
- 517 J. A. Veech. A probabilistic model for analysing species co-occurrence. *Global Ecology and Biogeography*, 22(2):252–260, 2013.
- 518 M. Vellend, M. Dornelas, L. Baeten, R. Beauséjour, C. D. Brown, P. De Frenne, S. C. Elmendorf, N. J. Gotelli, F. Moyes, I. H.
519 Myers-Smith, et al. Estimates of local biodiversity change over time stand up to scrutiny. *Ecology*, 98(2):583–590, 2017.

- 520 A. K. Winegardner, B. K. Jones, I. S. Ng, T. Siqueira, and K. Cottenie. The terminology of metacommunity ecology. *Trends*
521 *in ecology & evolution*, 27(5):253–254, 2012.
- 522 M. S. Wisz, J. Pottier, W. D. Kissling, L. Pellissier, J. Lenoir, C. F. Damgaard, C. F. Dormann, M. C. Forchhammer, J.-A.
523 Grytnes, A. Guisan, et al. The role of biotic interactions in shaping distributions and realised assemblages of species:
524 implications for species distribution modelling. *Biological reviews*, 88(1):15–30, 2013.
- 525 H. Xu, M. Detto, S. Fang, Y. Li, R. Zang, and S. Liu. Habitat hotspots of common and rare tropical species along climatic and
526 edaphic gradients. *Journal of Ecology*, 103(5):1325–1333, 2015.
- 527 P. Yodzis. The indeterminacy of ecological interactions as perceived through perturbation experiments. *Ecology*, 69(2):508–515,
528 1988.
- 529 K. Yoshida. Evolutionary dynamics of species diversity in an interaction web system. *Ecological Modelling*, 163(1-2):131–143,
530 2003.

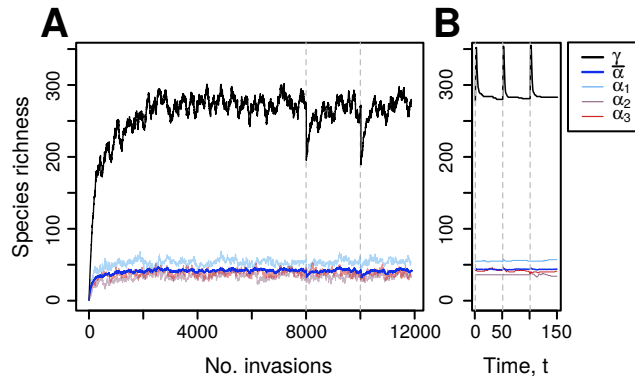


Figure 1: **Biodiversity regulation in model metacommunities.** The emergence of diversity equilibria at multiple spatial scales as a result of a stepwise invasion flux in a typical model metacommunity (A). Regional diversity (γ , black) and the average local diversity ($\bar{\alpha}$, blue) are shown, as well as that observed in three randomly selected patches (α , coloured). Relaxation back to equilibrium following random removal or introduction of large numbers of species (25% of the equilibrium richness, indicated by vertical dashed lines, A and B) reveals the strength and predictability of metacommunity-scale regulation in model assemblages. Relaxation times following removal and introduction differ by several orders of magnitude since the re-accumulation of diversity occurs at the invasion timescale, while extirpations occur at the population-dynamic timescale (measured in units t).

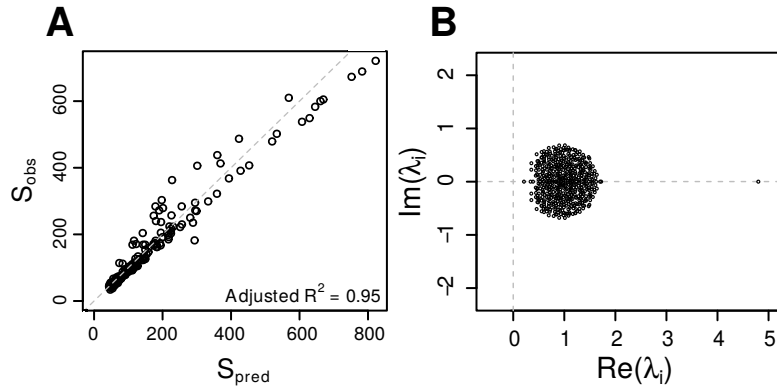


Figure 2: **Testing for biodiversity regulation by structural stability in metacommunity models.**

A: Comparison of the regional equilibrium diversity predicted by Eq. (2) and that observed in simulated metacommunities for 195 combinations of patch number and spatial heterogeneity. The dashed line signifies equality.

B: The eigenvalue spectrum of a typical regional-scale competitive overlap matrix **C**. Both analyses strongly suggest the mechanism regulating diversity at the metacommunity scale is the loss of ecological structural stability.

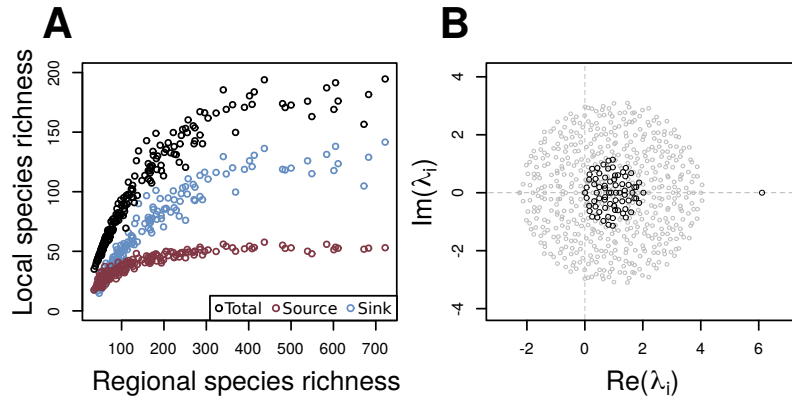


Figure 3: **Demonstration of structurally unstable diversity regulation at the local scale.** A: Average local diversity (black), and that attributed to source (red) and sink (blue) populations, at regional diversity equilibrium, plotted against regional species richness for the same 195 parameter combinations used in Fig. 2. The sublinearity of the local-regional richness relation suggests local communities are saturated with respect to both source and sink diversity for sufficiently high N . B: Comparison of the spectra of the full competitive overlap matrix \mathbf{A} (grey circles) with that of its sub-matrix matrix $\mathbf{A}_{\text{source}}$ (black circles) corresponding to source populations only, for a randomly selected local community at regional diversity equilibrium. The spectrum of $\mathbf{A}_{\text{source}}$ demonstrates the role of structural instability in regulating the diversity of the key, locally sustained component of the local assemblage.

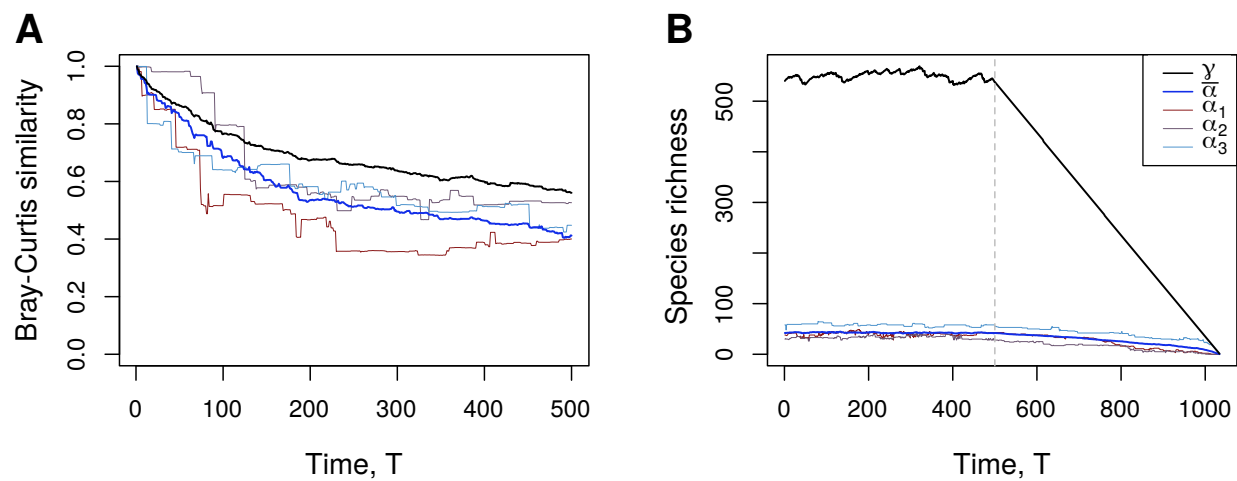


Figure 4: **Temporal trends in community composition and species richness of model communities.** The temporal Bray-Curtis similarity (A) and *source* population species richness (B, $T < 500$) for a metacommunity at regional equilibrium subject to a slow, discrete flux of invaders. Data for the metacommunity (black), the local average (blue) and three randomly selected local communities (coloured) are shown. After 500 invasions the invasion flux in panel (B) is switched off and species are successively removed in order of increasing regional abundance.

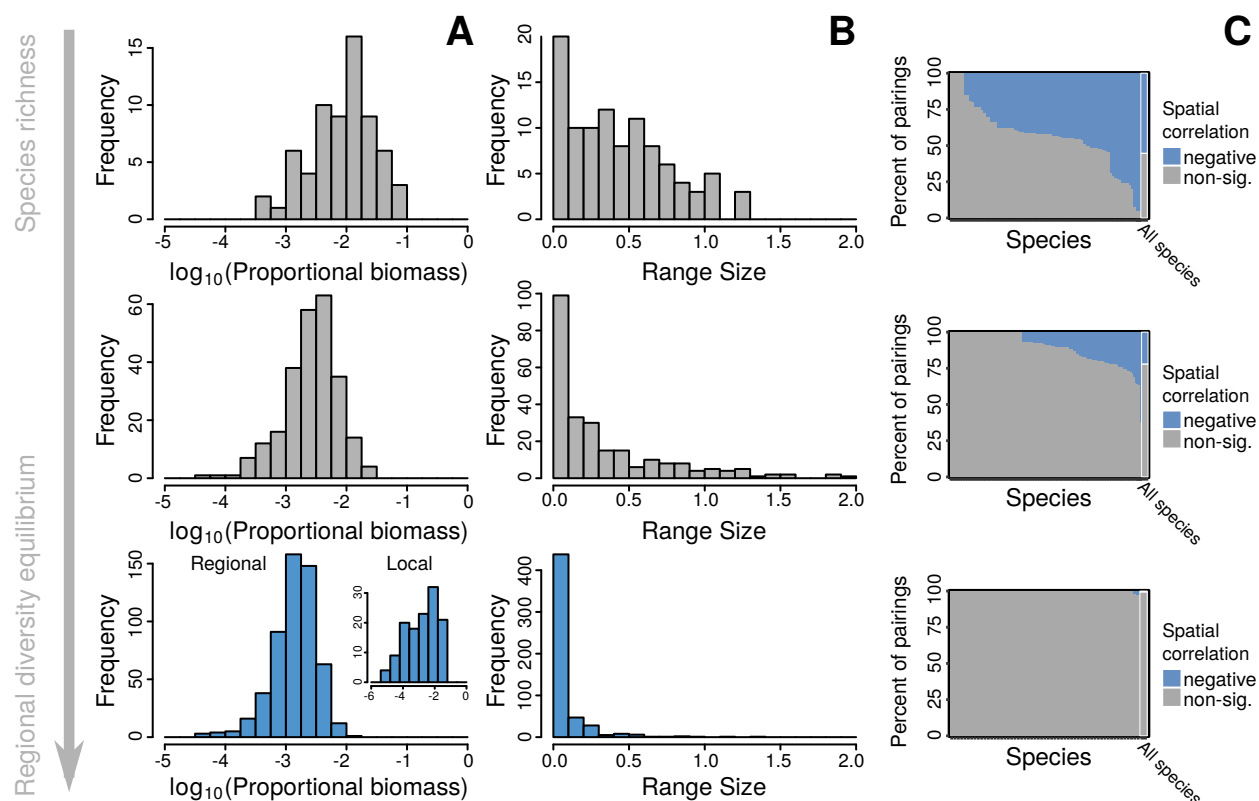


Figure 5: **The effect of regional diversity regulation on macroecology in simulated metacommunities.** Species Biomass Distributions (A), Range Size Distributions (B), and (C) Co-occurrence Profiles (Veech, 2006; Griffith et al., 2016) for a typical model metacommunity at 20, 50, and 100% of the regional diversity equilibrium of around 500 species. In B, an even distribution over the model landscape corresponds to a Range Size measure of 1.7, though for species concentrated near the edges our measure of Range Size can give even larger values. In C, the percentage of possible species pairs that exhibit statistically significant ($p < 0.05$) negative spatial correlation is shown in blue for each species, and for the community as a whole (right-most bar). Unsurprisingly, given the purely competitive nature of local ecological interactions, in our model metacommunities, no significant positive correlations were found. All three distributions converge on patterns well represented in the empirical literature as metacommunities approach the self-organized equilibrium.

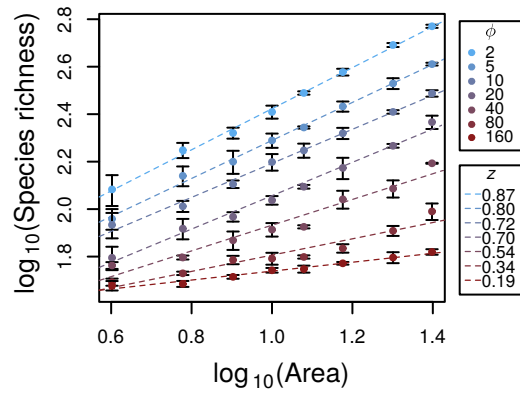


Figure 6: **Species area relations for simulated metacommunities.** Species richness increases as a function of model area according to approximate power laws with exponents ranging from 0.19 to 0.87. Colours indicate the degree of spatial environmental heterogeneity, ϕ . Error bars indicate standard deviations estimated from three independent model runs for each parameterization, for which small differences between simulations arose largely due to the random topography of the model landscapes.